Supplementary Information (SI) for New Journal of Chemistry.

Supporting Information

A MOFs–derived Fe-Cu@NC electrocatalyst for efficient conversion of nitrate into ammonia

Supporting Text

1. Chemicals

2-Methylimidazole ($C_4H_6N_2$), zinc nitrate hexahydrate ($Zn(NO_3)_2 \cdot 6H_2O$) ferric nitrate nonahydrate ($Fe(NO_3)_3 \cdot 9H_2O$), copper phthalocyanine ($C_{32}H_{16}CuN_8$), and copper(II) acetate monohydrate ($Cu(CH_3COO)_2 \cdot H_2O$) were obtained from Aladdin Reagent Co., Ltd. (Shanghai, China). Methanol (MeOH) was purchased from Sinopharm Chemical Reagent Co., Ltd. (Shanghai, China). Melamine ($C_3H_6N_6$) was purchased from Macklin Biochemical Co., Ltd. (Shanghai, China). Hydrochloric acid (HCl) was obtained from Beijing Tongguang Fine Chemicals Co., Ltd. (Beijing, China). Sodium hydroxide (NaOH) and sodium nitrate ($NaNO_3$) were obtained from Xilong Scientific Co., Ltd. (Shantou, China). Nessler's reagent ($HgCl_2$-KI-KOH) was obtained from Beijing Tongguang Weiye Technology Co., Ltd. (Beijing, China). All chemicals were analytical grade and used as received without further purification.

Supporting Table

Tab. S1 Relative proportions of different Cu oxidation states from the Cu LMM Auger spectra of Cu@NC and Fe-Cu@NC.

Sample	Cu^0			Cu^+		
	B.E. (eV)	area	fraction	B.E. (eV)	area	fraction
Cu@NC	567.98	16.97	6.81%	569.63	232.02	93.19%
Fe-Cu@NC	568.18	52.53	28.50%	569.83	131.61	71.50%

Tab. S2 A summary of CO-accessible site density and XPS-based Fe/Cu partition.

Sample	Fe-Cu@NC
Total CO uptake / total desorbed CO (μmol g^{-1})	11.943
Total CO-accessible sites (sites g^{-1})	7.19×10^{18}
Fe content determined by XPS (at.%)	0.15
Cu content determined by XPS (at.%)	0.19
Fe fraction for partition = Fe/(Fe+Cu)	0.441
Estimated Fe-accessible sites (μmol g^{-1})	5.27
Estimated Fe-accessible sites (sites g^{-1})	3.17×10^{18}
Estimated Cu-accessible sites (μmol g^{-1})	6.67
Estimated Cu-accessible sites (sites g^{-1})	4.02×10^{18}

Tab. S3 Adsorption energies (E_{ads}, eV) of adsorbed intermediates on different models/sites.

Adsorbate*	Cu@NC (Cu site)	Fe-Cu@NC (Cu site)	Fe-Cu@NC (Fe site)
$*NO_3$	-3.4125	-3.6309	-2.5261
*NHO	-1.6337	-2.1620	-2.2261
*H	-	0.4598	-0.5136

Tab. S4 Bader charge variation (Δe, e) of Cu atoms in Cu@NC and Fe-Cu@NC models.

Cu atom	Δe (Fe-Cu@NC) / e	Δe (Cu@NC) / e
Cu 1	-0.059906	-0.061359
Cu 2	0.002198	-0.016616
Cu 3	0.022441	-0.001651
Cu 4	-0.004030	-0.019151
Cu 5	0.022622	-0.005096
Cu 6	-0.157121	-0.067035
Cu 7	0.051691	0.035173
Cu 8	0.014947	0.001245
Sum (Cu 1 – Cu 8)	-0.107157	-0.134491
Mean (Cu 1 – Cu 8)	-0.013395	-0.016811

Tab. S5 Screening estimation of electricity demand for the 900 ℃ pyrolysis and associated CO_2 emission (Beijing grid factor).

Item	Unit	Value / Input	Notes
Rated furnace power, P	kW	3	Tube furnace rated power
Holding time at 900 ℃, t_{hold}	h	2	Holding step used in this work
Electricity for holding step, E_{hold}	kWh	6	Holding step only; excludes ramping and auxiliary loads
Grid emission factor, GEF (Beijing)	kg CO_2/kWh	0.5554[a]	Provincial average electricity CO_2 factor (published by MEE & NBS)
CO_2 from electricity, m_{CO2}	kg CO_2	3.33	$m_{CO_2} = E_{hold} \times GEF = 6 \times 0.5554$
Direct CO_2 intensity of conventional NH_3 production (IEA benchmark)	t CO_2/NH_3	2.4[b]	Direct-emission benchmark for context; not a full LCA comparison

Note: The table layout follows the SI reporting style commonly used for screening-level energy and carbon accounting in related electrocatalysis studies.[1-3]

[a] The location-based grid emission factor for Beijing (2023, 0.5554 kg CO_2/kWh), the most recent officially available value, is taken from the dataset released by the Ministry of Ecology and Environment (MEE) and the National Bureau of Statistics (NBS).

[b] The benchmark value (~2.4 t CO_2/NH_3) is adopted from the IEA "Ammonia Technology Roadmap" and is used for contextual comparison on a direct-emission basis.

Supporting Figure

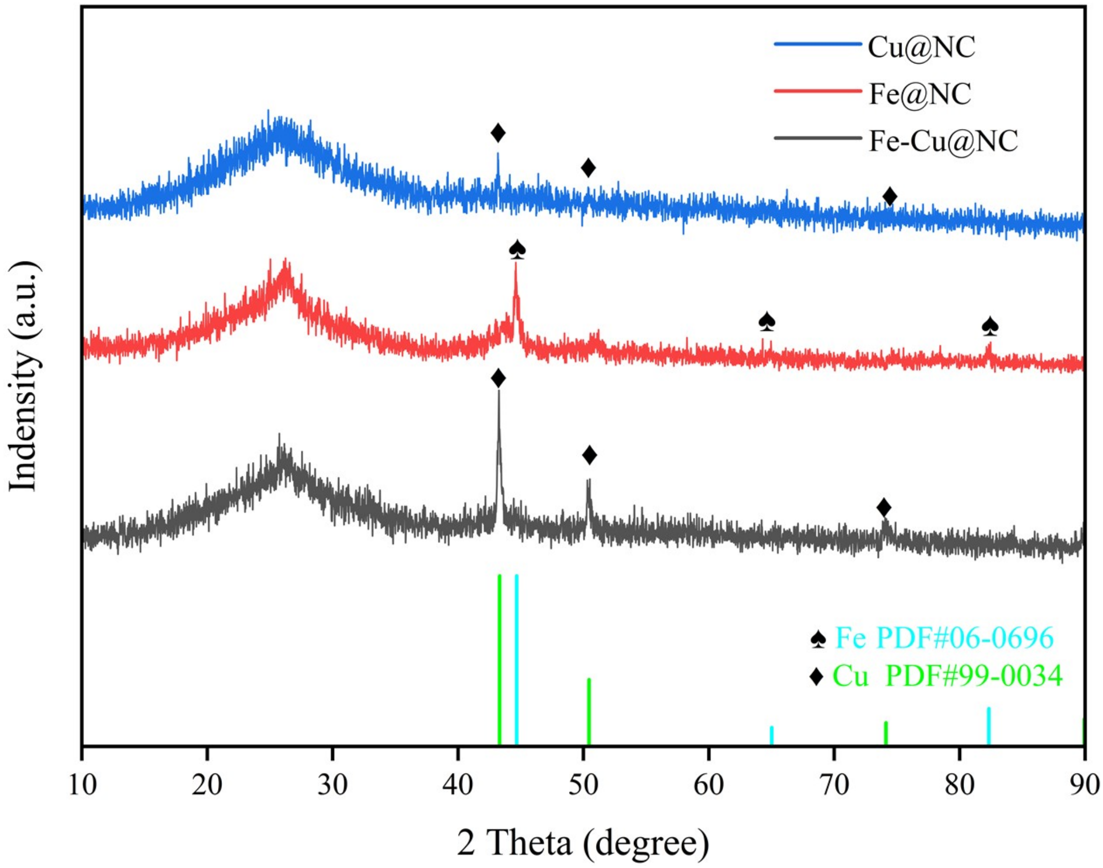

Fig. S1 XRD patterns of Cu@NC, Fe@NC, and Fe-Cu@NC.

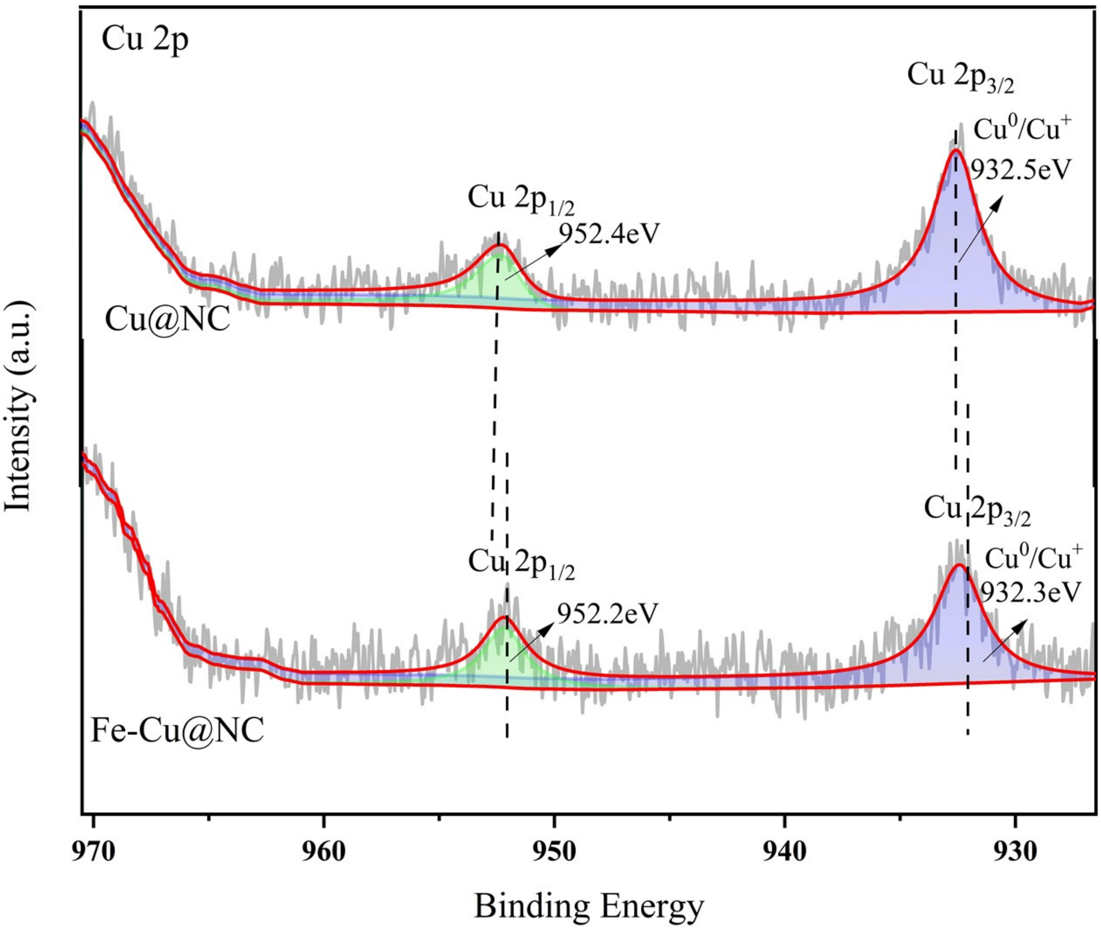

Fig. S2 Cu 2p spectra of Cu@NC and Fe-Cu@NC.

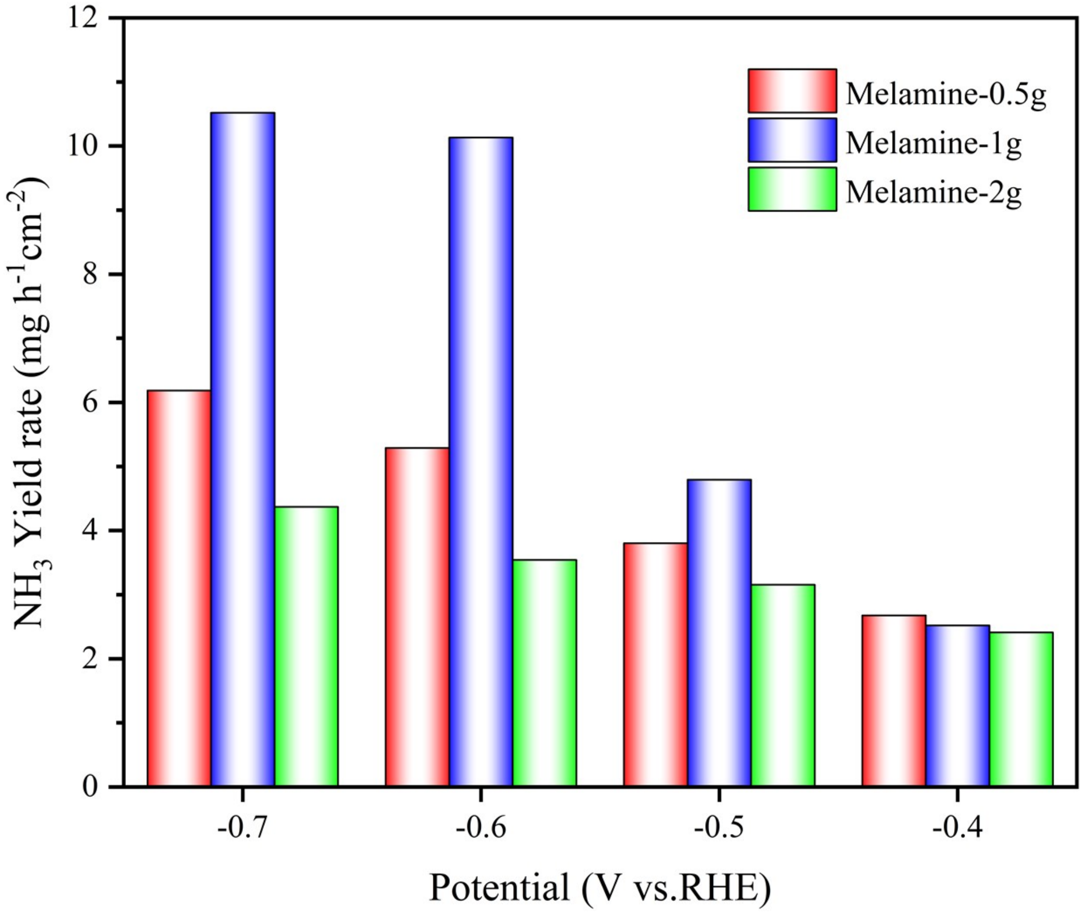

Fig. S3 Effect of N-doping level on NH_3 yield rate.

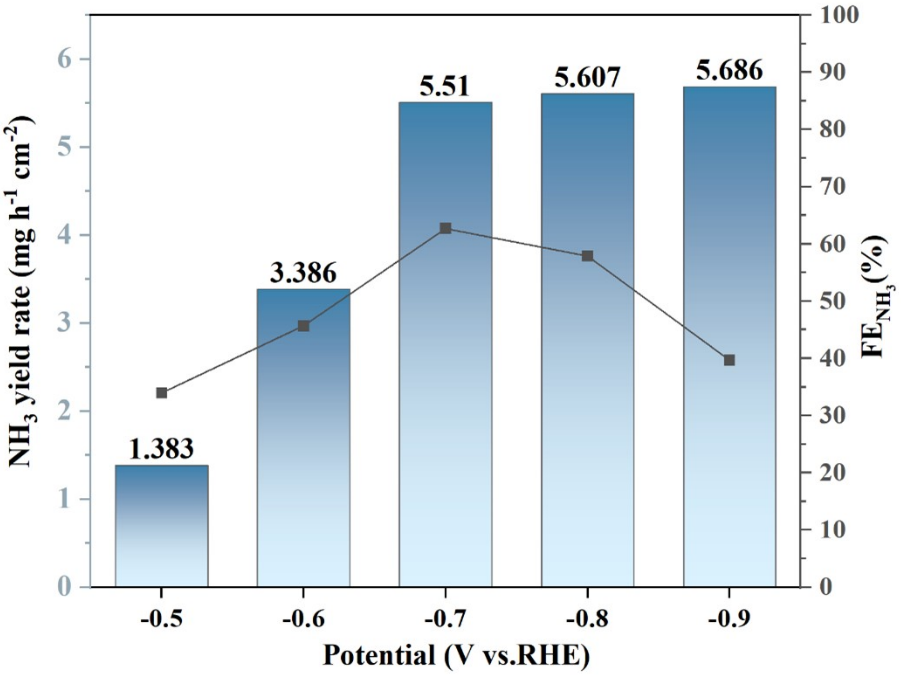

Fig. S4 NH_3 yield rate and Faradaic efficiency of the physically mixed Fe@NC+Cu@NC at different potentials.

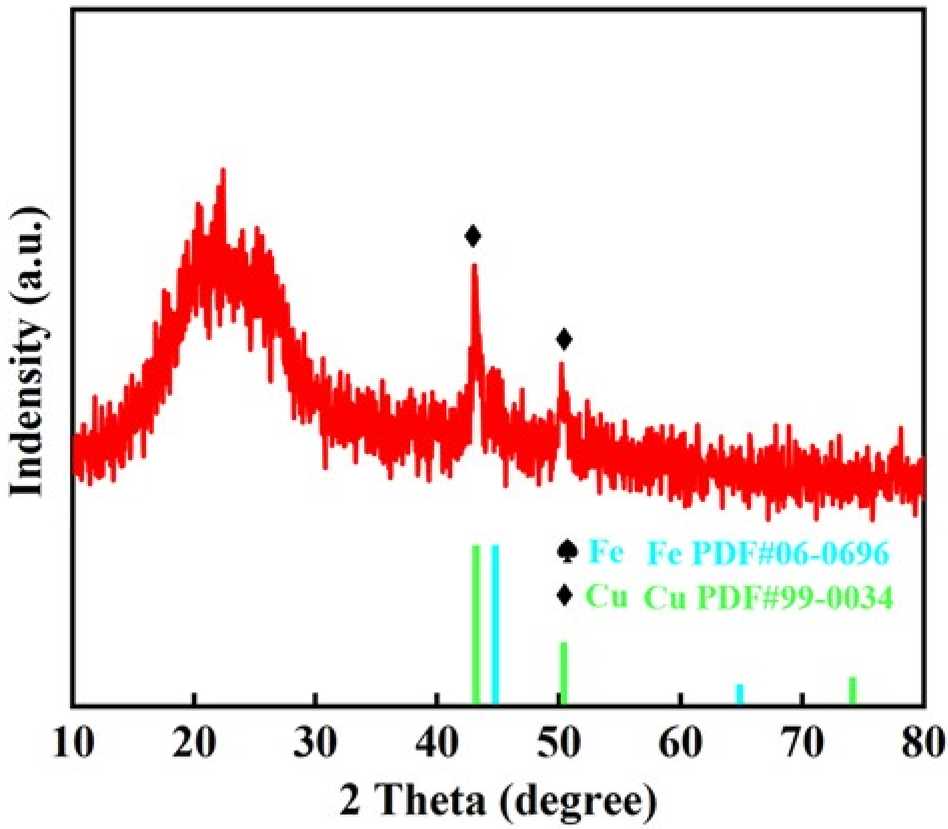

Fig. S5 XRD patterns of Fe-Cu@NC before and after the long-term stability test.

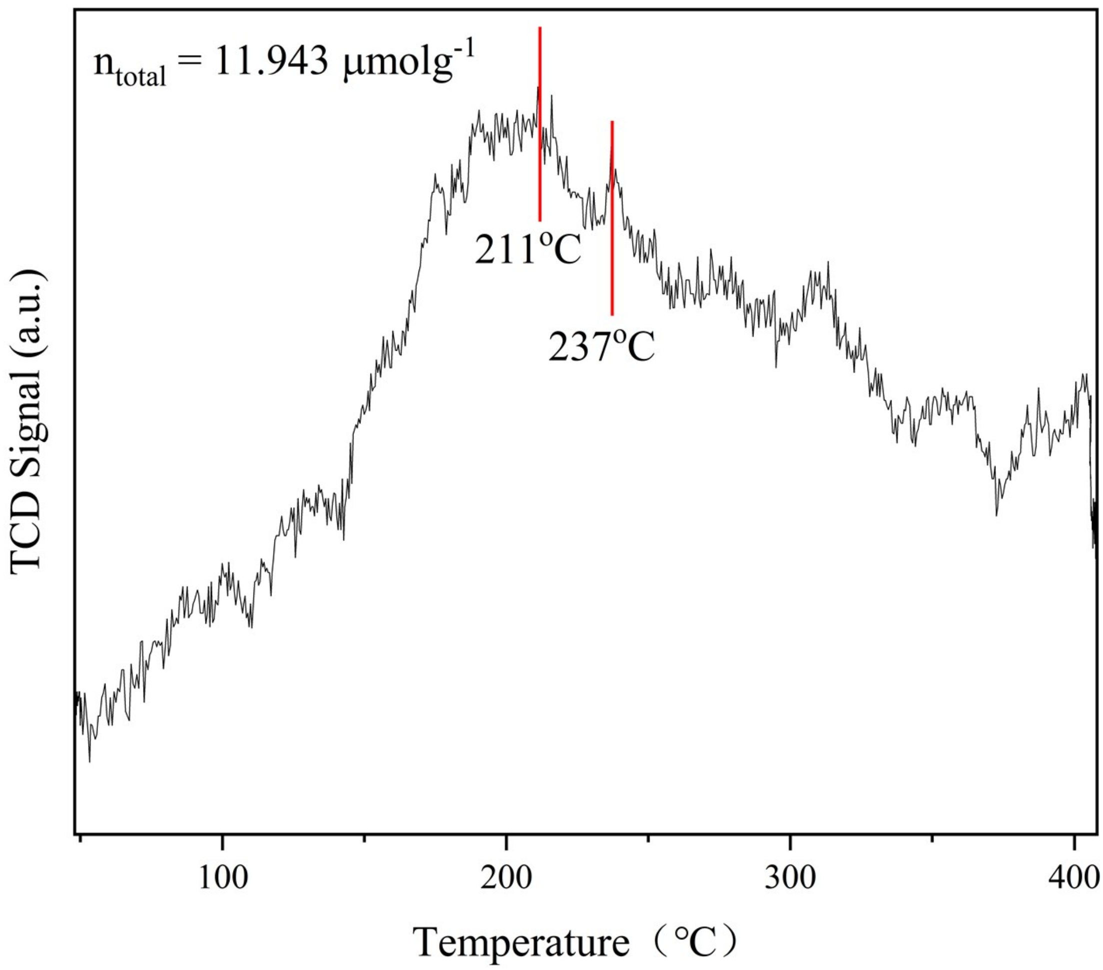

Fig. S6 CO-TPD profile of Fe-Cu@NC after CO adsorption.

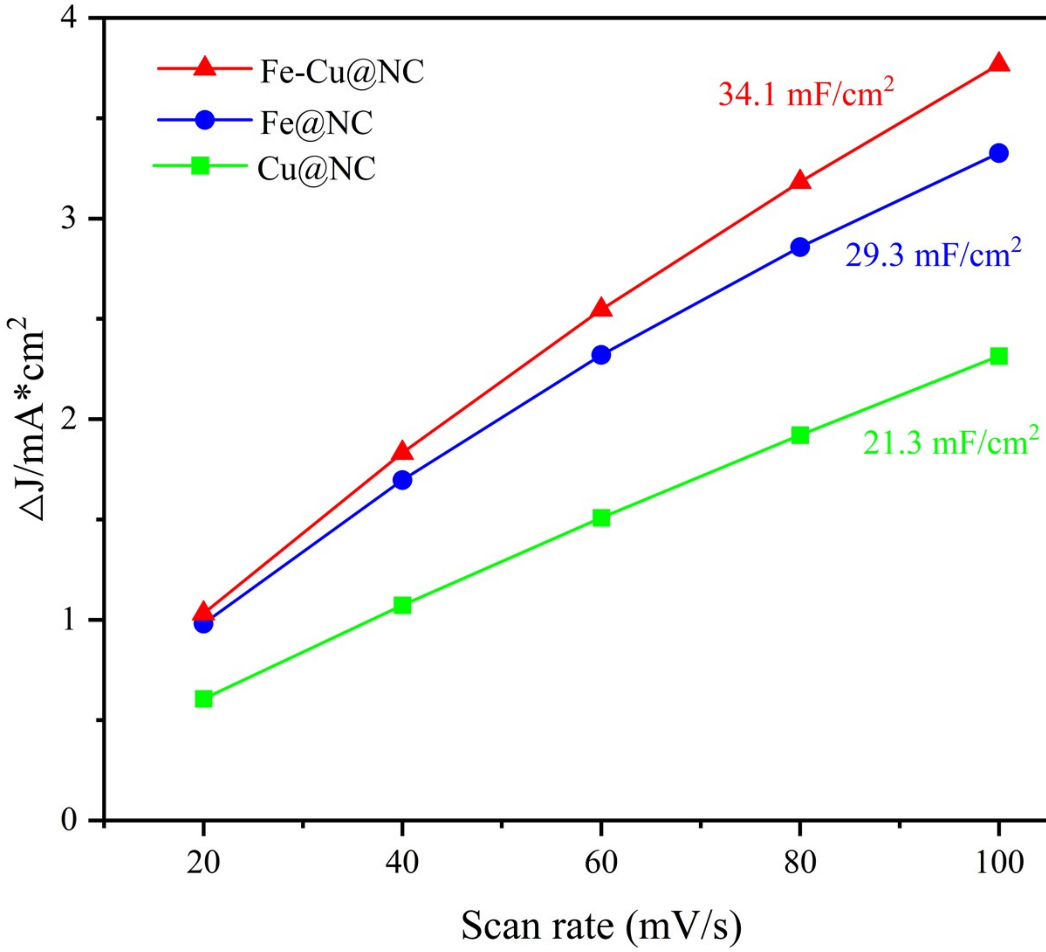

Fig. S7 Double-layer capacitance (Cdl) of Fe-Cu@NC, Fe@NC, and Cu@NC.

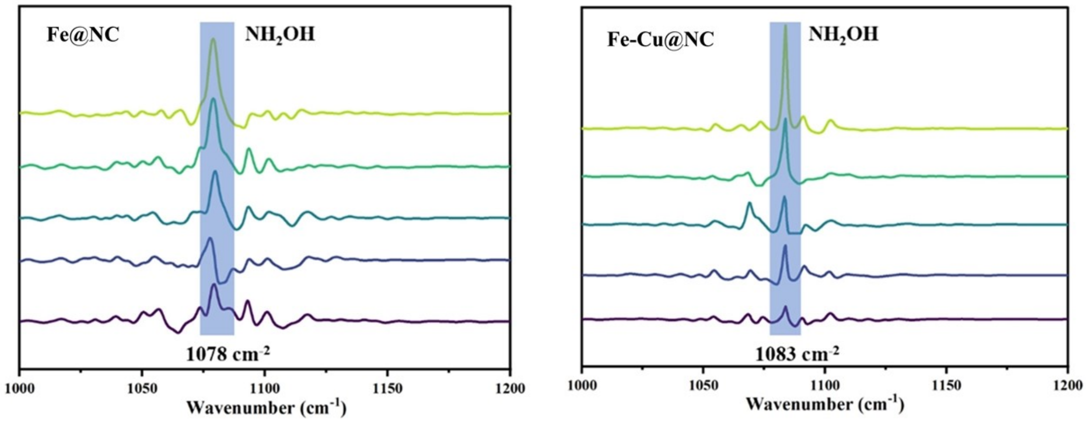

Fig. S8 Operando FTIR spectra of surface intermediates during NO_3RR over Fe@NC and Fe-Cu@NC.

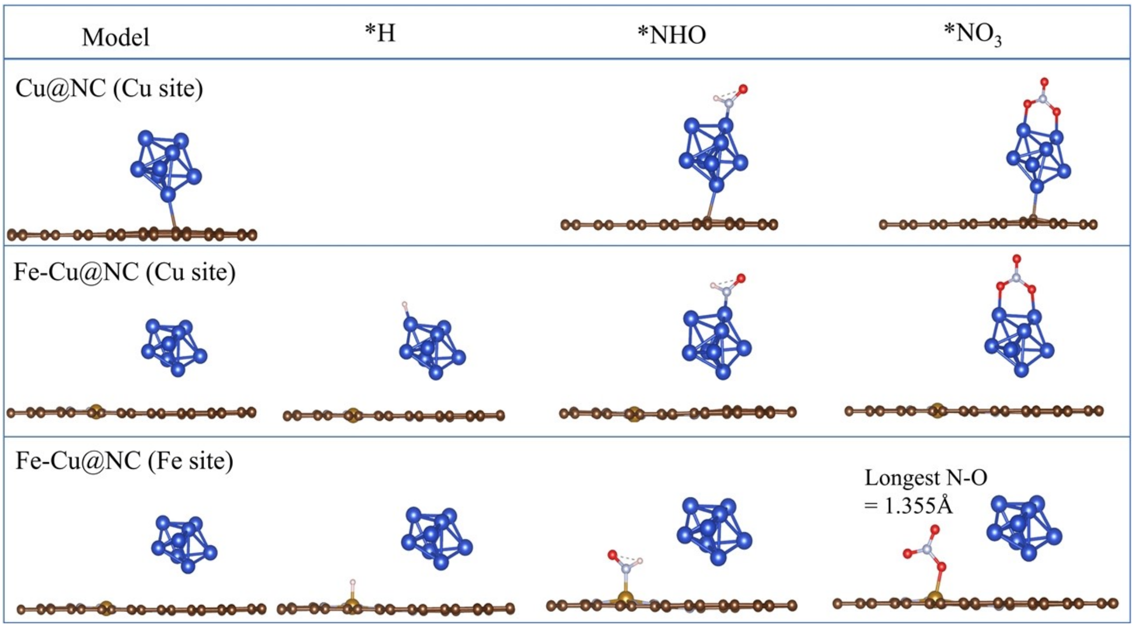

Fig. S9 Optimized adsorption configurations of key intermediates on Cu@NC and Fe-Cu@NC models.

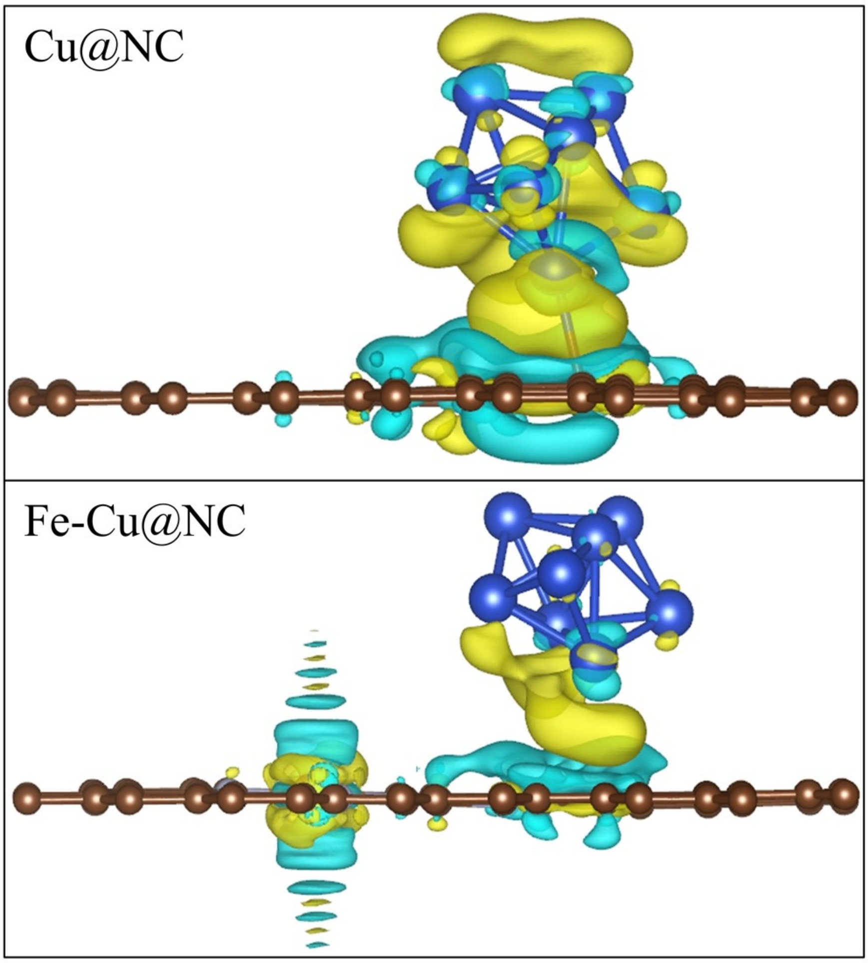

Fig. S10 Charge density difference (CDD) maps of Cu@NC model and Fe–Cu@NC model.

References

1. D. M. Miller, M. J. Liu, K. Abels, A. Kogler, K. S. Williams and W. A. Tarpeh, *Energy Environ. Sci.*, 2024, **17**, 5691-5705.
2. J. Y. Guo, M. J. Liu, C. Laguna, D. M. Miller, K. S. Williams, B. D. Clark, C. Muñoz, S. J. Blair, A. C. Nielander, T. F. Jaramillo and W. A. Tarpeh, *Energy Environ. Sci.*, 2024, **17**, 8787-8800.
3. R. Daiyan, T. Tran-Phu, P. Kumar, K. Iputera, Z. Z. Tong, J. Leverett, M. H. A. Khan, A. A. Esmailpour, A. Jalili, M. Lim, A. Tricoli, R. S. Liu, X. Y. Lu, E. Lovell and R. Amal, *Energy Environ. Sci.*, 2021, **14**, 3588-3598.